Design of novel neurokinin 1 receptor antagonists based on conformationally constrained aromatic amino acids and discovery of a potent chimeric opioid agonist-neurokinin 1 receptor antagonist

Steven Ballet[1], **Debby Feytens**[1], **Koen Buysse**[1], **Nga N. Chung**[2], **Carole Lemieux**[2], **Suneeta Tumati**[3], **Attila Keresztes**[3], **Joost Van Duppen**[4], **Josephine Lai**[3], **Eva Varga**[3], **Frank Porreca**[3], **Peter W. Schiller**[2], **Jozef Vanden Broeck**[4], and **Dirk Tourwé**[1]

[1] Department of Organic Chemistry, Vrije Universiteit Brussel, Brussels, Belgium

[2] Department of Chemical Biology and Peptide Research, Clinical Research Institute, Montreal, Canada

[3] Department of Pharmacology, University of Arizona, Tucson, AZ, U.S.A

[4] Animal Physiology and Neurobiology, Zoological Institute, Katholieke Universiteit Leuven, Leuven, Belgium

Abstract

A screening of conformationally constrained aromatic amino acids as base cores for the preparation of new NK1 receptor antagonists resulted in the discovery of three new NK1 receptor antagonists, **19** [Ac-Aba-Gly-NH-3′,5′-(CF$_3$)$_2$-Bn], **20** [Ac-Aba-Gly-NMe-3′,5′-(CF$_3$)$_2$-Bn] and **23** [Ac-Tic-NMe-3′,5′-(CF$_3$)$_2$-Bn], which were able to counteract the agonist effect of substance P, the endogenous ligand of NK1R. The most active NK1 antagonist of the series, **20** [Ac-Aba-Gly-NMe-3′,5′-(CF$_3$)$_2$-Bn], was then used in the design of a novel, potent chimeric opioid agonist-NK1 receptor antagonist, **35** [Dmt-D-Arg-Aba-Gly-NMe-3′,5′-(CF$_3$)$_2$-Bn], which combines the *N*-terminus of the established Dmt^1-DALDA agonist opioid pharmacophore (H-Dmt-D-Arg-Phe-Lys-NH$_2$) and **20,** the NK1R ligand. The opioid component of the chimeric compound **35,** i.e. Dmt-D-Arg-Aba-Gly-NH$_2$ **36**, also proved to be an extremely potent and balanced μ- and δ opioid receptor agonist with subnanomolar binding and in vitro functional activity.

Keywords

NK1 receptor antagonists; opioids; multitarget drug design; designed multiple ligands

Introduction

Substance P (SP, Arg-Pro-Lys-Pro-Gln-Gln-Phe-Phe-Gly-Leu-Met-NH$_2$), an undecapeptide neurotransmitter or neuromodulator, is a member of the tachykinin family of peptides. These peptides mediate their biological functions through binding to three neurokinin G protein-coupled receptors, NK1, NK2 and NK3, which have as endogenous ligands the peptides SP,

neurokinin A and neurokinin B, respectively.[1] The NK1 receptor is expressed both in the CNS and in peripheral tissues. The observation that the release of SP is linked to the transmission of pain and inflammatory responses related to noxious stimuli,[2] makes SP receptor antagonists (NK1R antagonists) potential therapeutic agents for pathologies such as postoperative pain, migraine,[3] arthritis,[4] asthma, nausea and emesis.[1,5,6]

Small peptidomimetic NK1R antagonists have been developed and often possess a bis-aromatic motif, typically consisting of a substituted (-OMe or -bis-CF$_3$) phenyl group next to another aromatic ring that is coupled to a central scaffold (e.g. **1**–**4**, Figure 1).[7–9] The relative disposition of the aromatics in such ligands was investigated in a large set of SP antagonists and resulted in a hypothesis for the receptor-bound conformation of NK1R antagonists.[9,10] In most cases, the two aromatic groups, crucial for high receptor affinity, are in proximity of each other and are proposed to adopt either a parallel face-to-face[9] or a perpendicular "T" or edge-on "L" arrangement. [10]

Biologically, prolonged pain states lead to neuroplastic changes in the CNS that modify/increase the release of certain neurotransmitters, such as the pronociceptive neurotransmitter SP, and increase the expression of the corresponding receptors for these released pain-enhancing ligands.[11–13] The current treatment of chronic pain cannot counteract these changes and hence the currently used analgesics are not effective in these pathological conditions. For this reason, an approach was taken to design bifunctional ligands that act as agonists at opioid receptors and as antagonists at NK1 receptors.[11,16,17,18] The concept for this type of designed multiple ligand (DML)[19] was originally developed by Lipkowski and coworkers.[18,20–22] Antagonism at the NK1 receptors blocks the signals induced by SP, the native ligand for NK1R, and would potentially inhibit the increased secretion of the peptide hormone SP and the enhanced expression of NK1 receptors upon sustained opioid administration or in prolonged pain states, while the opioid subunit of these DMLs, on the other hand, would be responsible for the activation of μ-opioid (MOR) and δ-opioid (DOR) receptors to produce the analgesic effect. Moreover, the administration of morphine to NK1 knockout mice did not show the morphine-related rewarding properties.[23]

In general, the advantages of multitarget agents include enhanced efficacy, relative to drugs that use the "one active agent, one target" approach by modulating multiple targets simultaneously and lower risk of drug-drug interaction which can potentially cause unexpected side-effects and/or toxicity. Because poor safety and a lack in efficacy are the main causes of failure of compounds in clinical trials, the approach of multitarget drug discovery is a research area of increasing interest in drug discovery programs.[24] Other advantages of a single ligand with multiple biological activities over a cocktail of individual drugs are: i) easy administration, ii) single biodistribution, iii) simple pharmacokinetic profile, and iv) higher concentrations at the synaptic cleft, which may lead to significant synergies in potency and efficacy.[24]

Hruby and Lipkowski synthesized three lead chimeras, **6** (TY 027, [H-Tyr-D-Ala-Gly-Phe-Met-Pro-Leu-Trp-NH-3′,5′-Bn(CF$_3$)$_2$]), **7** (H-Tyr-D-Ala-Gly-Phe-Met-Pro-Leu-Trp-O-3′,5′-Bn(CF$_3$)$_2$) and **8** (H-Tyr D-Ala-Gly-Phe-NH-NH-Trp-Cbz) (Figure 2), that contain an enkephalin-based opioid pharmacophore at the N-terminus and a NK1 receptor-binding subunit at the C-terminus.[11,16,22,24–27] Gratifyingly, the dual opioid-NK1R activity resulted in both enhanced antinociception in acute pain models and prevention of opioid-induced tolerance in chronic trials for the peptidic bifunctional ligand **6** and its ester analog **7**.[16,25] Compounds **6** and **7** were shown to potently attenuate neuropathic pain without producing opioid-induced tolerance and hence they seem to validate the concept or approach of using bifunctional opioid agonist-NK1 antagonist chimeras to tackle this type of pathology. [28]

Previously, we have suggested the 4-amino-1,2,4,5-tetrahydro-2-benzazepin-3-one **9** (Aba) and amino indoloazepinone **10** (Aia) (Figure 3) to represent *privileged templates*. The appropriate derivatization of the central core scaffolds **9** and **10** allowed to obtain (selective) ligands for several G protein-coupled receptors. Examples include: opioid GPCRs,[29,30] bradykinin B$_2$[31] and somatostatin receptors.[32,33]

In this work we present the 3′,5′-bistrifluoromethyl benzyl derivatization of the conformationally constrained amino acids Aba **9** and Aia **10** and, in addition, of the tetrahydroisoquinoline-3-carboxylic acid (Tic) **11** tetrahydro-β-carboline-3-carboxylic acid (Tcc) **12** templates for the development of new NK1R antagonists. The 1-phenyl-benzazepine core **9** (R$_1$ = Ph) was chosen as an alternative for the benzodiazepine core in **4** (Figure 1),[14] whereas the indoloazepine core **10** could be considered to lead to a constrained analogue of the potent antagonist **5**.[15]

The biological evaluation of all newly prepared compounds for NK1R antagonism, led to the identification of 3 potent antagonists. This discovery allowed us to integrate the novel NK1R pharmacophore into the design of a compact peptidomimetic bifunctional opioid-NK1R ligand containing an opioid agonist component derived from the potent μ opioid agonist [Dmt^1]DALDA (H-Dmt-D-Arg-Phe-Lys-NH$_2$; Dmt = 2′,6′-tyrosine).[34] Here, we present the design rationale, synthesis and *in vitro* biological evaluation of both NK1R ligands and a dual opioid-NK1R ligand.

Results and Discussion

Synthesis

Using an earlier reported methodology the Phth-(1*S/R*)-(4*S*)-amino-1,2,4,5-tetrahydro-2-benzazepin-3-ones stereoisomers **13** and **14** were obtained.[35]

N-methyl-3′,5′-bistrifluoromethyl benzylamine was prepared by *N*-methylation of the corresponding, commercially available, benzyl chloride.[36] Coupling of this secondary amine, or the primary 3′,5′-bistrifluoromethyl benzylamine, with TBTU as a coupling reagent in the presence of Et$_3$N gave the *N*-protected Phth-(1*R*)-4-amino-(4*S/R*)-benzazepinone intermediates. Removal of the phthaloyl protective group via hydrazinolysis was completed in refluxing EtOH and followed by a standard acetylation using acetic acid anhydride and DIPEA as a base. The final compounds **15** to **17** were purified by preparative RP-HPLC followed by lyophilization (purity ≥ 95%).

These compounds were structurally analogous to investigated benzodiazepines of type **4** (Figure 1) that possessed the desired NK1R antagonism.[14] In this benzodiazepine series, as described by Armour et al., the role and necessity of the third aromatic moiety was questioned and this motivated us to make the compounds without the 1-phenyl substitution (Scheme 2). As mentioned in the introduction, numerous examples of NK1R antagonists containing only two aromatics are published (selected examples: **1** to **3** and **5** in Figure 1).

We started from the dipeptide mimetic Boc-(S)-Aba-Gly-OH **18**[37] which was again coupled to both *N*-methyl- and 3′-5′-bistrifluoromethyl benzylamine. Removal of the Boc group by classic acidolysis (TFA/CH$_2$Cl$_2$/anisole 49:49:2) and acetylation, followed by HPLC purification, gave aminobenzazepinones **19** and **20**. The identical pathway starting from commercial Boc-(S)-Tic-OH **21** yielded tetrahydroisoquinoline analogues **22** and **23**.

The seven- and six-membered Trp-based constrained Aia and Tcc analogues were prepared from the Boc-2′-formyl-(*S/R*)-Trp-OH **24a/b**[32] and Boc-(*S/R*)-Tcc-OH **25a/b**,[38] respectively (Scheme 3). Reductive amination with methyl glycinate and sodium cyanoborohydride was

immediately followed by EDC-mediated lactamization. The latter reaction was slow and needed 48h to give complete conversion to **26a/b**. Saponification with LiOH and standard coupling using TBTU gave **27a/b**. The final acetylated structures **28a/b** were obtained using the procedure for the Aba and Tic ligands, after acidolysis and treatment with acetic anhydride.

A constrained analogue of **5** (Ac-Trp-O-3′,5′-(CF$_3$)$_2$Bn,[39] Figure 1) was synthesized starting from **24a** via reductive alkylation with 3′,5′-bistrifluoromethyl benzylamine and carbodiimide–induced cyclization, to afford indoloazepinone **29**. Standard Boc deprotection and acetylation gave **30**. Moreover, both (*S*)- and (*R*)-Tcc derivatized structures **32a** and **32b** were obtained after a coupling/deprotection/acetylation sequence similar to that used for the Tic-analogues **22** and **23**. Finally, the chimeric opioid-NK1R DML **35** (Scheme 4) was prepared after identification of the most potent NK1R antagonist, proven to be compound **20** (see section Biological evaluation). For the synthesis of the double pharmacophore-containing peptidomimetic structure we combined an adapted (constrained) version of Dmt^1-[DALDA] (Dmt-D-Arg-Phe-Lys-NH$_2$) with **20**. As such, the N-terminal fragment Boc-Dmt-D-Arg(Pbf)-Aba-Gly-OH was first prepared using a Fmoc solid phase peptide synthesis strategy on 2-chlorotrityl resin with DIC as a coupling reagent and HOBt as an additive (Scheme 4). Boc-Dmt-OH was coupled as the final residue, so that the *N*-terminal Boc group would be cleaved simultaneously with the acid labile Pbf side-chain protective group. First, the protected sequence Boc-Dmt-D-Arg(Pbf)-Aba-Gly-OH 33 was removed from the 2-Cl-trityl resin under mild acidic conditions (1% TFA in CH$_2$Cl$_2$ for 30 min). Introduction of the C-terminal pharmacophoric unit, the *N*-methyl-3′,5′-bistrifluoromethyl benzylamide, was performed by a coupling the secondary amine with **33** by means of BOP in the presence of diisopropylethylamine in dichloromethane over 3h at room temperature. Final cleavage of the protection groups in **34** was achieved by treatment with TFA/CH$_2$Cl$_2$ 49/49 (2h at r.t.) and anisole (2%) to scavenge the released carbocations during deprotection. The final compound **35** was purified by preparative HPLC (≥95% purity).

The peptidic sequence for verification of the opioid activity of the *N*-terminal opioid component, H-Dmt-D-Arg-Aba-Gly-NH$_2$ **36**, was prepared by standard SPPS using Nα-Fmoc chemistry on Rink resin with DIC/HOBt as the coupling mixture (not shown). After cleavage from the solid support, the solvent was removed in vacuo, the resulting crude mixture was washed with chilled Et$_2$O, and the precipitate purified via preparative HPLC.

Biological Evaluation and Structure-Activity Relationships

The functional activity of the potential NK1 receptor ligands was evaluated for NK1R agonism and antagonism using an assay measuring the agonist-induced calcium-dependent aequorine-luminescence of cells expressing NK1 receptors.[40]

None of the derivatized 1-phenyl-Aba- (Scheme 1), Aba- and Tic- (Scheme 2), and Aia- and Tcc-analogues (Scheme 3) showed any significant agonism up to a concentration of 10^{-4}M (not shown). This is in contrast to SP which gave the expected NK1R activation and served as the positive agonist control compound. Next, the targeted neurokinin 1 receptor antagonism of all compounds was evaluated. Three compounds (**19, 20** and **23**) were able to counteract the effect of SP, as proven by the rightward shift of the dose-response curve of SP in the functional receptor assay (see supporting information for graphical data).

These results demonstrate that both Tic and Aba can serve as a core scaffold for the development of NK1R antagonists and that for the Aba-type central scaffolds, the 1-phenyl substituent hinders antagonism at N1KR for both (4*S*)- and (4*R*) configurations (**15–17**). In contrast, the constrained tryptophan analogues **28a/b**, **30** and **32a/b**, obtained by derivatization of both **24a/b** and **25a/b**, did not show any antagonist properties. This

indicates that these types of conformational constraints are not mimicking the bioactive conformation of **5** or that the change of the ester function in **5** into an amide function is not tolerated. These structural features are however also present in the most potent NK1R antagonist in the series, analogue **20**. The preferred conformations of **20** was studied by molecular modeling using Macromodel.[54] The three lowest energy conformations which differ by only 4.72 kJ/mol, have orientations of the aromatic rings corresponding to the stacked (Figure 4A), the perpendicular T- (Figure 4B) or L-orientations (Figure 4C).[9,10] The distances between the centroids of the aromatic rings (4.25, 5.33 and 5.49 Å, respectively) are within the range proposed for 3′,5′-bistrifluoromethyl benzyl-containing NK1R antagonists.[10] This suggests that **20** is able to orient its aromatic rings for the most efficient interaction with the NK1R. In the indole analogue of **20**, compound **28a**, similar conformations were found. However, the pyrrole ring in **28a** shifts the annulated benzene ring to a further distance from the 3′,5′-bistrifluoromethyl benzene ring than in **20**. This might account for the difference in NK1R antagonist potency.

The calculated pA_2 values (Table 1) allowed to rank the relative potency of the Aba- and Tic-derived structures **19**, **20** and **23**.[41,42] These values indicate that a *N*-methylation at the level of the C-terminal amide bond resulted in improved antagonist activity [pA_2(**19**) = 6.2 vs. pA_2(**20**) = 8.4 and pA_2(**23**) = 7.5] and that the lactam constraint of **20**, in combination with the carboxymethyl chain of Gly, was favored over the isoquinoline constraint in **23**.

In a next step, the binding affinity (K_i) of the active compounds was determined on CHO membranes expressing the human NK_1 receptor. These data show that the antagonist potency, indicated as pA_2, of these compounds is in accordance with the receptor binding affinities and gives the relative rank order of **19** < **23** < **20**. The moderate nanomolar binding affinity of **19** and lack of antagonism of **22** offers proof that, for compounds of type **19–20** and **22–23**, the presence of a hydrogen bond donor at the C-terminal benzyl amide, is unfavorable for receptor binding and antagonist activity. Both **20** and **23** possess a tertiary amide linkage which results in increased hydrophobicity and eliminates the possibility for hydrogen bond formation at the amide bond site.

Earlier results have demonstrated that the use of the Aba scaffold in opioid peptides results in very potent agonists with high receptor affinity.[30,43–45] Several examples were reported in which Aba serves as the third residue in synthetic peptidic opioid ligands (e.g. Tyr[1]-D-Ala[2]-Aba[3]-Gly[4]-NH$_2$,[39] Tyr[1]-D-Ala[2]-Aba[3]-Gly[4]-Tyr[5]-Pro[6]-Ser[7]-NH$_2$.[46] This conformational constraint yields a substantial enhancement in DOR affinity, while maintaining MOR binding and functional activity. In addition, the presence of a positive charge in the side chain of a D-Arg residue in position 2 is suggested to play a role in the excellent membrane transport properties of Dmt [1]-D-Arg[2]-Phe[3]-Lys[4]-NH$_2$.[47,48] For these reasons, we prepared the opioid 'control' compound Dmt-D-Arg-Aba-Gly-NH$_2$ **36** via solid phase peptide synthesis using Fmoc chemistry with Rink amide resin as a solid support. As can be seen from Table 1 both the opioid receptor affinities and functional activities of **36** are extremely high and balanced for the μ- and δ-receptor, as indicated by subnanomolar values in all assays. On the other hand, this compound showed weak receptor binding affinity. These data also indicate that D-Arg in position 2 can be combined with the conformational constraint imposed by Aba[3] to provide a potent and balanced μ/d opioid component for the DML.

The *framework combination*[24] of potent ligands for the two separate targets resulted in multitarget ligand **35**, which is a combination of the most potent NK1R antagonist of the series, Ac-Aba-Gly-NMe-3′,5′-(CF$_3$)$_2$Bn **20**, and the very potent opioid ligand Dmt-D-Arg-Aba-Gly-NH$_2$ **36**. Although a modest loss in NK1R antagonism was observed for **35** (pA_2 8.4 → 7.8), subnanomolar hNK1R binding (K_i 0.5 nM) was determined and proves that the presence of the opioid subunit even adds favorable features for efficient binding to this G

protein-coupled receptor. As for the opioid in vitro characteristics, one can see that MOR binding is less disrupted, compared to DOR affinity, when both frameworks are combined. A three-fold loss in μ opioid receptor -but still subnanomolar- binding affinity was determined ($K_i(\mu)$ 0.15 → 0.416 nM), whereas a 17-fold loss in DOR affinity was observed ($K_i(\delta)$ 0.6 → 10.4 nM), relative to the opioid 'control' compound **36**. As expected on the basis of the weak receptor binding affinity of **36**, chimera **35** showed weak κ receptor binding affinity as well. The receptor binding affinities are in agreement with the results obtained in the *in vitro* functional GPI and MVD tissue bioassays. In the guinea pig ileum assay, reflecting mainly μ opioid receptor activation, a low nanomolar IC_{50} value of 8.51 nM indicates that, even though a potency loss is observed relative to **36**, DML **35** still is a very potent agonist at the opioid μ receptor. The results of the MVD assay indicate that DOR agonist activity is still maintained but only with a two digit nanomolar IC_{50} value.

The creation of bifunctional ligands of the type of compound **35** in general is a difficult task because the connected pharmacophores can interfere with each other to change or reduce their binding and activity at the corresponding target receptors. Therefore the merged DML **35** is a very successful example of a dual ligand in which a large overlap of pharmacophores is present. The central Aba structure is part of both pharmacophores. In addition, our earlier research had shown that a benzyl amide moiety was tolerated in the shorter opioid ligand Dmt-Aba-Gly-NH- Bn for both MOR and DOR,[30] although this subunit was shifted by one position (D-Arg in position 2 is inserted) in hybrid **35** described here.

Conclusions

Different constrained Phe and Trp amino acid mimics were used as central scaffolds in the design of new NK1R analogues. Unfortunately, all Trp-derivatives were inactive, both as agonists and antagonists, in the functional assay measuring the agonist-induced calcium-dependent aequorine- luminescence of cells expressing NK1 receptors. Gratifyingly, the derivatization of the Ac-Tic and Ac-Aba-Gly scaffolds as the 3′,5′-bistrifluoromethyl benzylamides resulted in moderate (structure **19**) to good (structures **20** and **23**) NK1R antagonists. The commonality of the Aba ring in both opioid and NK1R ligands, prompted us to combine both pharmacophores and produce successfully a compact bifunctional opioid-NK1R ligand (structure **35**) that targets both the opioid and the neurokinin system. This study also identified opioid control compound **36**, as an extremely potent and balanced μ- and δ opioid receptor agonist in vitro, which deserves further investigation.

Chimeric ligand **35** can be considered as a small DML with highly merged frameworks. In general medicinal chemists try to maximize the degree of overlap, and hence minimize molecular weight, in order to have a better chance at oral activity.[24] Ongoing research consists of the structural fine-tuning of this new lead compound. More extensive *in vitro* and *in vivo* assays are scheduled to verify the membrane permeability of this dual opioid agonist-NK1 receptor antagonist through important biological barriers, such as the blood-brain barrier (BBB).

Experimental section

General

Thin layer chromatography (TLC) was performed on plastic sheet pre-coated with silica gel $60F_{254}$ (Merck, Darmstadt, Germany) using specified solvent systems. Mass Spectrometry (MS) was recorded on a Micromass Q-Tof Micro spectrometer using electrospray (ESP) ionization (positive or negative ion mode). Data collection was done with Masslynx software. Analytical RP-HPLC was performed using an Agilent 1100 Series system (Waldbronn, Germany) with a Supelco Discovery BIO Wide Pore® (Bellefonte, PA, USA)

RP C-18 column (25 cm × 4.6 mm, 5 μm) using UV detection at 215 nm. The mobile phase (water/acetonitrile) contained 0.1% TFA. The gradient consisted of a 20 min run from 3 to 97% acetonitrile at a flow rate of 1mL/min. Preparative HPLC was performed on a Gilson apparatus and controlled with the software package Unipoint. The Reverse Phase C18-column (Discovery BIO Wide Pore 25 cm × 21.2 mm, 10 μm) was used under the same conditions as the analytical RP-HPLC, but with a flow rate of 20 mL min^{-1}. A purity of more than 95% was determined for all compounds by analytical RP-HPLC using the conditions described above. ^{1}H-NMR and ^{13}C-NMR spectra were recorded at 250 MHz and 63 MHz, respectively, on a Bruker Avance 250 spectrometer or at 500 MHz and 125 MHz on a Bruker Avance II 500. Calibration was done with TMS (tetramethylsilane) or residual solvent signals as an internal standard. The solvent used is mentioned in all cases and the abbreviations used are: s (singlet), d (doublet), dd (double doublet), t (triplet), br s (broad singlet), m (multiplet).

Functional NK1R assay[40]

Cell line and cell culture conditions—The Chinese Hamster Ovary K1 (CHO-K1) cell line, stably expressing human NK1 receptor (hereafter referred to as CHO-NK1 cells), was transfected with an apoaequorin expression vector (pER2) using Fugene6 (Roche Applied Science). The cell line and expression vector were obtained from Euroscreen (Belgium). The CHO-NK1 cells were cultured in sterile DMEM/HAM's F12 medium (Sigma) supplemented with 10% foetal bovine serum, 100 IU/ml penicillin, 100 μg/ml streptomycin and 400 μg/ml G 418 (Geneticin, Gibco), at 37°C with 5% CO_2 and were trypsinized every 3 days.

Aequorin charging protocol—Transfected cells in the mid-log phase were detached by changing the growth medium for PBS buffer supplemented with 5mM EDTA (pH 8). The cells were spun down and incubated for 4h at a concentration of 5×10^6 cells/ml in DMEM-F12 medium without phenol red (Gibco) supplemented with 0.1% BSA (BSA-medium) and 5 μM coelenterazine h (Molecular Probes). After coelenterazine loading, the cells were diluted 10-fold in the same medium and incubated for an additional period of 30 minutes. The cells were mildly shaken during the incubation periods.

Aequorin luminescence assay—A dilution series of peptide agonist (Substance P was purchased from Sigma) ranging from 10^{-11} to 10^{-4} M was distributed in a white 96-well plate. For investigating antagonism, the synthetic compounds were added to these wells to obtain the desired concentrations (ranging from 10^{-8} to 10^{-4} M). One negative control sample (BSA medium only) was included in each row of the 96-well plate. The plate was loaded in a "Multimode Reader Mithras, LB940" (Berthold). The wells were screened one by one and each measurement started at the moment of injection of 50μl of the coelenterazine-loaded cell suspension, containing 2.5×10^4 cells. Light emission was measured every second for 30s after which 50μl of 10nM ATP solution (positive control) was injected. Each measurement was carried out in duplicate. Light emission was recorded for an additional period of 10s per well and the data were presented in Relative Light Units (RLU).

Data Analysis—Luminescence data (peak integration) were calculated using MikroWin 2000 software (Berthold), which was linked to the Microsoft Excel program. All statistical and curve-fitting analyses were performed using Prism 4.0 (GraphPad) software. Data are expressed in percentage (% RLU) of the maximal luminescence that was detected with 10^{-4} M SP (without antagonist). The competitive nature of antagonism was evaluated using the Schild plot method.[41] All antagonists analyzed in this study provided linear regression plots

and were considered competitive. The pA_2 values were calculated using the Schild's equation.[42]

hNK1/CHO cell membrane preparation and Radioligand binding assay

Recombinant hNK1/CHO cells were grown to confluency in 37 °C, 95% air and 5% CO_2, humidified atmosphere, in a Forma Scientific (Thermo Forma, OH, USA) incubator in Ham's F12 medium supplemented with 10% fetal bovine serum, 100 U/ml penicillin,100 μg/ml streptomycin and 500 μg/ml Geneticin. The confluent cell monolayers were then washed with Ca^{2+}, Mg^{2+}-deficient phosphate-buffered saline (PD buffer) and harvested in the same buffer containing 0.02% EDTA. After centrifugation at 2700 rpm for 12 min, the cells were homogenized in ice-cold 10 mM Tris-HCl and 1 mM EDTA, pH 7.4 buffer. A crude membrane fraction was collected by centrifugation at 18,000 rpm for 12 min at 4°C and the pellet was suspended in 50mM Tris-Mg buffer and protein concentration of the membrane preparation was determined by using Bradford assay.

Six different concentrations of the test compound were each incubated, in duplicates, with 20 μg of membrane homogenate and 0.4 nM [^{3}H] substance P (135 Ci/mmol, Perkin-Elmer, USA) in 1 mL final volume of assay buffer (50 mM Tris, pH 7.4, containing 5 mM $MgCl_2$, 50 μg/mL bacitracin, 30 μM bestatin, 10 μM captopril, and 100 μM phenylmethylsulfonylfluoride) Substance P at 10 μM was used to define the nonspecific binding. The samples were incubated in a shaking water bath at 25 °C for 20 min. The [^{3}H] substance P concentration and the incubation time was selected based on the studies of Yamamoto et al.[26] The reaction was terminated by rapid filtration through Whatman grade GF/B filter paper (Gaithersburg, MD, USA) presoaked in 1% polyethyleneimine, washed 4 times each with 2 mL of cold saline, and the filter bound radioactivity was determined by liquid scintillation counting (Beckman LS5000 TD). The media and chemicals listed above were purchased from Sigma (Sigma-Aldrich, St. Louis, MO, USA) unless otherwise stated.

Data analysis

Analysis of data collected from three independent experiments performed in duplicates is done using GraphPad Prizm 4 software (GraphPad, San Diego, California). Log IC_{50} values for each test compound were determined from nonlinear regression. The inhibition constant (K_i) was calculated from the antilogarithmic IC_{50} value by the Cheng and Prusoff equation.[49]

Functional GPI and MVD assays

The guinea pig ileum (GPI)[50] and mouse vas deferens (MVD)[51] bioassays were carried out as described in detail elsewhere. [52,53] A dose-response curve was determined with [Leu^5]enkephalin as standard for each ileum and vas preparation and IC_{50} values of the compounds being tested were normalized according to a published procedure.[54]

Opioid receptor binding assays

Opioid receptor binding studies were performed as described in detail elsewhere.[52] Binding affinities for μ and δ opioid receptors were determined by displacing, respectively, [^{3}H]DAMGO (Multiple Peptide Systems, San Diego, CA) and [^{3}H]DSLET (Multiple Peptide Systems) from rat brain membrane binding sites, and κ opioid receptor binding affinities were measured by displacement of [^{3}H]U69,593 (Amersham) from guinea pig brain membrane binding sites. Incubations were performed for 2 h at 0 °C with [^{3}H]DAMGO, [^{3}H]DSLET and [^{3}H]U69,593 at respective concentrations of 0.72, 0.78 and 0.80 nM. IC_{50} values were determined form log-dose displacement curves, and K_i values were calculated from the IC_{50} values by means of the equation of Cheng and Prusoff,[49]

using values of 1.3, 2.6 and 2.9 nM for the dissociation constants of [^{3}H]DAMGO, [^{3}H]DSLET and [^{3}H]U69,593, respectively.

Molecular Modeling

The calculations were carried out using Macromodel 5.0[54] with Maestro 8.0 as a graphic interface. The MM3* force field[55] was used for energy minimization in combination with the GB/SA solvation model of Still *et al.*,[56] using MacroModel's default parameters for an aqueous medium. Conformational searches were carried out using the Pure Low Mode Search.[57] Structures were generated and minimized by means of the Polak-Ribière conjugate gradient method as implemented in MacroModel, using a gradient convergence criterion of 0.1 kJ/mol Å. The resulting conformations were again minimized to an energy convergence of 0.01 kJ/mol Å. Duplicate structures and those greater than 50kJ/mol above the global minimum were discarded. The remaining structures were clustered into families using Xcluster 1.7 (the aromatic carbons were used as comparison atoms). A RMSD value of 0.2 Å was used.

General synthetic procedures

Boc deprotection—Boc-protected amine (1.8 mmol) was dissolved in a mixture of TFA:water 95:5 (13 mL) and acetonitrile was added (6 mL). The reaction was stirred for 1 h and the mixture was evaporated. Crude TFA salts were used in the next reactions.

Formation of amide bonds—Carboxylic acid (54 mmol) was dissolved in dry CH_2Cl_2 (250 mL). NEt_3 (22.5 mL, 162 mmol, 3 equiv) and TBTU (19.07 g, 59 mmol, 1.1 equiv) were added and the mixture was stirred at room temperature for 10 min. Amine TFA salt (59 mmol, 1.1 equiv) was added and the pH was kept at 8 by the addition of NEt_3. The reaction was stirred for 1 h. The solution was extracted with HCl (1M, 3×80 mL), $NaHCO_3$ (saturated, 3×80 mL) and brine (3×80 mL). The organic layer was dried over $MgSO_4$ and after filtration, the residue was evaporated. No further purification was necessary.

Acetylation—Amine TFA salt (0.89 mmol, 1 equiv) was dissolved in acetonitrile:water 1:1 (10 mL) and the pH was adjusted to 6 by the addition of NEt_3. Ac_2O (0.42 mL, 4.5 mmol, 5 equiv) was added in three portions while the pH was kept at 6. The reaction was stirred during 2 h at room temperature. The solution was evaporated and after the addition of EtOAc (25 mL), it was extracted with HCl (1M, 3×15 mL), $NaHCO_3$ (saturated, 3×15 mL) and brine (3×15 mL). The organic layer was dried over $MgSO_4$ and after filtration, the solution was evaporated.

Saponification—Methyl ester (4.1 mmol) was dissolved in MeOH (96 mL) and aqueous LiOH (1M, 4 equiv, 16 mmol, 16.2 mL) was added. The reaction was monitored by TLC (silica, EtOAc) and after 1.5 h it was complete. MeOH was evaporated, and water (100 mL) and EtOAc (50 mL) were added. After extraction, the aqueous layer was acidified to pH4 and extracted with EtOAc (3× 50 mL). The organic layers were combined and washed with brine (3× 100 mL). The organic phase was dried over $MgSO_4$ and after filtration, the mixture was evaporated.

Peptide synthesis—Peptide **36** was synthesized manually by N^a-Fmoc solid phase methodology on Rink amide resin (0.189 mmol scale) using DIC and HOBt as the coupling reagents. A threefold excess of the building blocks (Fmoc-Aba-Gly-OH, Fmoc-D-Arg(Pbf)-OH and Fmoc-Dmt-OH) and activating agents was applied in the presence of a ninefold excess of diisopropylethylamine and dry DMF was used as a solvent. Fmoc-deprotections were carried out by treating the resin twice (5 min and 15 min) with 20% piperidine in DMF. Final cleavage of the peptide as well as the Pbf side chain protection group removal

was accomplished by treatment with TFA/TES/water 90:5:5 for 90 minutes. The peptide was isolated and purified by RP-HPLC on a SUPELCO DiscoveryBIO wide pore preparative C18 column in 45% overall yield and was >95% pure as determined by analytical RP-HPLC. The structure of pure compound **36** was confirmed by high-resolution electrospray ionization (ESP) mass-spectrometry.

Hybrid **35** was prepared through a two-step approach. First, Boc-Dmt-D-Arg(Pbf)-Aba-Gly-OH was prepared on 2-chlorotrityl resin (0.15 mmol). Fmoc-Aba-Gly-OH (1.2 equiv) and DIPEA (5 equiv) in CH_2Cl_2 were added to the swollen solid support and the reaction mixture was shaken overnight. The resin was washed three times with DMF, and three times with CH_2Cl_2. Subsequently, Fmoc-D-Arg(Pbf)-OH and Boc-Dmt-OH were coupled as described above. The protected C-terminal free acid Boc-Dmt-D-Arg(Pbf)-Aba-Gly-OH **33** was obtained after treatment of the resin with 1% v/v TFA in CH_2Cl_2 for 30 min. The obtained crude peptide was obtained after removal of the solvent in vacuo. The crude peptide was pure enough to be used directly in the second step, the coupling step with *N*-methyl-3′,5′-bistrifluoromethyl benzylamine. This reaction was carried out on **33** (0.043mmol) in CH_2Cl_2 (10mL) after adding BOP (1.1 equiv) in the presence of DIPEA (2.5 equiv), and using CH_2Cl_2 as a solvent. After stirring the reaction mixture for 3h, an extraction with saturated sodium bicarbonate (5mL) was performed and the organic phase was dried over magnesium sulphate and the solvent was removed. After final treatment with TFA/CH_2Cl_2/anisole 49:49:2 for 2h, evaporation of the solvent under vacuum yielded crude compound **35** which was purified and characterized by preparative RP-HPLC and HRMS as mentioned above.

Compound characterization

Boc-(S)-Aba-Gly-NH-3′,5′-(CF₃)₂-Bn—Flash chromatography (EtOAc/Hexane 1:1) yielded the desired compound (white solid, 83%). HPLC (standard gradient): t_{Ret} 19.3 min; TLC R_f (EtOAc/hexane 1:1): 0.43; MS (ESP+) found m/z 560 [M + H]⁺, $C_{26}H_{27}F_6N_3O_4$ requires 559.19, ¹H NMR 250 MHz (CDCl₃): δ 7.78 (s, 1H), 7.65 (s, 2H), 7.30–7.02 (m, 4H), 6.72 (br s, 1H), 5.73 (d, 1H, *J* = 7.2 Hz), 5.29 (m, 2H), 4.44 (t, 2H, *J* = 6.5 Hz), 4.28 (d, 1H, *J* = 15.8 Hz), 4.07 (d, 1H, *J* = 15.8 Hz), 3.45 (dd, 1H, J_1 = 17.2 Hz, J_2 = 5.0 Hz), 2.96 (dd, 1H, J_1 = 17.3 Hz, J_2 = 14.4 Hz), 1.45 (s, 9H). ¹³C NMR (CDCl₃) δ 173.0, 168.8, 155.3, 140.6, 135.2, 132.6, 132.1, 131.7, 130.9, 128.8, 128.6, 127.8, 126.6, 121.5, 80.4, 53.6, 52.6, 50.4, 42.6, 36.9, 28.5

Ac-(S)-Aba-Gly-NH-3′,5′-(CF₃)₂-Bn 19—Preparative HPLC yielded the desired compound (white powder, 43%). HPLC (standard gradient): t_{Ret} 15.85 min; TLC R_f (EtOAc): 0.39; MS (ESP+) found m/z 502.14 [M + H]⁺, $C_{23}H_{21}F_6N_3O_3$ requires 501.15, ¹H NMR 250 MHz (CDCl₃): δ 8.27 (br s, 1H), 7.78 (m, 3H), 7.37–6.99 (m, 5H), 5.41 (m, 1H), 5.29 (d, 1H, *J* = 16.8 Hz), 4.53 (m, 3H), 4.00 (d, 1H, *J* = 16.8 Hz), 3.79 (d, 1H, *J* = 16.8 Hz), 3.45 (dd, 1H, J_1 = 17.7 Hz, J_2 = 5.5 Hz), 2.95 (dd, 1H, J_1 = 17.3 Hz, J_2 = 13.7 Hz), 2.04 (s, 3H). ¹³C NMR (CDCl₃) δ 171.8, 169.0, 168.2, 141.2, 135.0, 132.4, 131.2, 130.6, 130.3, 128.2, 127.6, 127.3, 125.7, 120.3, 52.6, 50.9, 48.3, 41.6, 35.7, 22.6

Boc-(S)-Aba-Gly-NMe-3′,5′-(CF₃)₂-Bn—After flash chromatography (EtOAc/Hexane 1:1) the desired compound was obtained (white solid, 81%). HPLC (standard gradient): t_{Ret} 18.9 min; TLC R_f (EtOAc/hexane 1:1): 0.49; MS (ESP+) found m/z 574 [M + H]⁺, $C_{27}H_{29}F_6N_3O_4$ requires 573.21, ¹H NMR 250 MHz (CDCl₃): δ 7.81 (s, 1H), 7.66 (s, 2H), 7.00–7.25 (m, 4H), 5.89 (d, 1H, *J* = 5.3 Hz), 5.34 (d, 1H, *J* = 15.9 Hz), 5.26 (m, 1H), 4.78 (s, 1H), 4.71 (s, 1H), 4.51 (d, 1H, *J* = 15.9 Hz), 4.00 (m, 2H), 3.51 (dd, 1H, J_1 = 16 Hz and J_2 = 4.4 Hz), 3.02 (m, 1H), 2.96 (s, 3H), 1.47 (s, 9H). ¹³C NMR (CDCl₃) δ 173.1, 168.5, 155.2,

139.3, 135.7, 132.4, 132.7, 131.9, 130.9, 128.6, 128.1, 126.5, 126.2, 121.8, 79.9, 53.2, 51.0, 49.5, 49.3, 37.2, 34.7, 28.3

Ac-(S)-Aba-Gly-NMe-3′,5′-(CF$_3$)$_2$-Bn 20—Preparative HPLC yielded the desired compound **20** (white powder, 47%). HPLC (standard gradient): t$_{Ret}$ 15.69 min; TLC R$_f$ (EtOAc/hexane 1:1): 0.40; MS (ESP+) found m/z 516 [M + H]$^+$, C$_{24}$H$_{23}$F$_6$N$_3$O$_3$ requires 515.16, ^{1}H NMR 250 MHz (CDCl$_3$): δ 7.82 (s, 1H), 7.69 (d, 2H), 7.31–6.96 (m, 4H), 5.49 (m, 1H), 5.36 (d, 1H, *J*=17.2 Hz), 4.80 (d, 1H, *J*=7.2 Hz), 4.74 (d, 1H, *J*= 7.2 Hz), 4.51 (d, 1H, *J*=17.2 Hz,), 4.51 (d, 1H, *J*= 17.0 Hz), 3.99 (m, 2H), 3.58 (dd, 1H, *J$_1$*= 17.6 Hz, *J$_2$*= 5.6 Hz), 2.98 (s, 3H), 2.10 (s, 3H). ^{13}C NMR (CDCl$_3$) δ 172.2, 170.2, 168.2, 139.3, 135.5, 132.4, 132.5, 131.9, 131.0, 128.6, 128.3, 128.0, 126.3, 121.4, 53.5, 51.0, 48.7, 49.5, 36.3, 34.8, 23.1

Boc-Tic-NMe-3′,5′-(CF$_3$)$_2$-Bn—After flash chromatography (EtOAc/Hexane 1:1) the desired compound was obtained with a yield of 90% (white solid, 65 mg). HPLC (standard gradient): t$_{Ret}$ 19.85 min; TLC R$_f$ (EtOAc/hexane 1:1): 0.75; MS (ESP+) found m/z 517 [M + H]$^+$, C$_{25}$H$_{26}$F$_6$N$_2$O$_3$ requires 516.18, ^{1}H NMR 250 MHz (CDCl$_3$): δ(*cis/trans*) 7.80 (s, 1H), 7.68 (s, 2H), 7.07–7.25 (m, 4H), 5.31 (t, 1H, *J* = 5.5 Hz), 5.15 (t, 1H, *J* = 5.5 Hz), 4.80 (m, 2H), 4.53 (m, 2H), 3.14 (s, 3H), 3.05 (m, 2H), 1.50 and 1.37 (2s, 9H). ^{13}C NMR (CDCl$_3$) δ(*cis/trans*) 172.6, 155.2, 140.0, 134.4, 132.1, 131.8, 128.4, 127.8, 127.0, 126.7, 125.8, 124.3, 121.4, 80.7, 50.8, 50.7, 46.0, 45.0, 35.2, 34.9, 31.2, 29.8, 28.3

Ac-Tic-NMe-3′,5′-(CF$_3$)$_2$-Bn 23—Purification was performed by preparative HPLC (51%, white powder). HPLC (standard gradient): t$_{Ret}$ 16.82 min; TLC R$_f$ (EtOAc/hexane 1:1): 0.72; MS (ESP+) found m/z 459 [M + H]$^+$, C$_{22}$H$_{20}$F$_6$N$_2$O$_2$ requires 458.14, ^{1}H NMR 250 MHz (CDCl$_3$): δ(*cis/trans* mixture) 7.77 (s, 1H), 7.65 (s, 2H), 7.29–7.14 (m, 4H), 5.41 (pseudo t, 1H, *J* = 6.0 Hz), 4.80–4.63 (m, 4H), 3.18 (s, 3H), 3.12 (m, 2H), 2.26 (s, 3H). ^{13}C NMR (CDCl$_3$) δ(*cis/trans* mixture) 172.4, 170.6, 139.8, 133.7, 132.9, 132.7, 130.5, 127.9, 127.8, 127.0, 125.6, 121.5, 51.8, 50.4, 47.4, 35.6, 30.9, 21.8

H-Dmt-D-Arg-Aba-Gly-NH$_2$ 36—Preparative HPLC yielded the desired compound (white powder, 45%). HPLC (standard gradient): t $_{Ret}$ 8.73 min; TLC R$_f$ (EBAW): 0.19; HRMS (ESP+) found m/z 581.3199 [M+H]$^+$, C$_{29}$H$_{41}$N$_8$O$_5$ requires 581.3195.

H-Dmt-D-Arg-Aba-Gly-NMe-3′,5′-(CF$_3$)$_2$Bn 35—Preparative HPLC yielded the desired compound (white powder, 54%). HPLC (standard gradient): t$_{Ret}$ 14.19 min; TLC R$_f$ (EBAW): 0.33; HRMS (ESP+) found m/z 821.3580 [M+H]$^+$, C$_{39}$H$_{47}$F$_6$N$_8$O$_5$ requires 821.3574.

Supplementary Material

Refer to Web version on PubMed Central for supplementary material.

Acknowledgments

Abbreviations

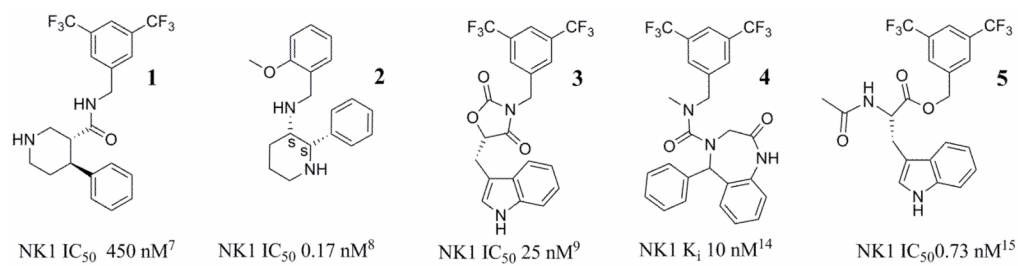|	
Aba	4-amino-1,2,4,5-tetrahydro-2-benzazepin-3-one
Aia	4-amino-1,2,4,5-tetrahydro-indolo[2,3-c]azepin-3-one
CHO cells	Chinese hamster ovary cells
CNS	central nervous system
DML	designed multiple ligand
DOR	δ opioid receptor
EBAW, ethyl acetate/n-butanol/ acetic acid/water 1	1:1:1 (v/v)
EDC	1-ethyl-3-(3-dimethylaminopropyl) carbodiimide
KOR	κ opioid receptor
MOR	μ opioid receptor
NK1R	neurokinin 1 receptor
SP	substance P
TBTU	O-(Benzotriazol-1-yl)-*N,N,N′,N′*-tetramethyluronium tetrafluoroborate
Tcc	1,2,3,4-tetrahydro-β-carboline-3-carboxylic acid
Tic	1,2,3,4-tetrahydroisoquinoline-3-carboxylic acid
Pbf	2,2,4,6,7-pentamethyldihydrobenzofuran-5-sulfonyl
Phth	phthaloyl

References

1. Longmore J, Hill RG, Hargreaves RJ. Neurokinin-Receptor Antagonists: Pharmacological Tools and Therapeutic Drugs. Can J Physiol Pharm. 1997; 75:612–621.

2. Maggi CA, Patacchini R, Rovero P, Giachetti A. Tachykinin Receptors and Tachykinin Receptor Antagonists. Autonomic Pharmacol. 1993; 13:23–93.

3. Moskowitz MA. Neurogenic Versus Vascular Mechanisms of Sumatriptan And Ergot Alkaloids in Migraine. Trends Pharmacol Sci. 1992; 13:307–311. [PubMed: 1329294]

4. Lotz M, Carson DA, Vaughan JH. Substance-P Activation of Rheumatoid Synoviocytes – Neural Pathway in Pathogenesis of Arthritis. Science. 1987; 235:893–895. [PubMed: 2433770]

5. Leroy V, Mauser P, Gao Z, Peet NP. Neurokinin Receptor Antagonists. Exp Opin Invest Drugs. 2000; 9:735–746.

6. Tattersall FD, Rycroft W, Francis B, Pearce D, Merchant K, MacLeod AM, Ladduwahetty T, Keown L, Swain C, Baker R, Cascieri M, Ber E, MacIntyre DE, Hill RG, Hargreaves RJ. Tachykinin NK$_1$ Receptor Antagonists Act Centrally to Inhibit Emesis Induced By The Chemotherapeutic Agent Cisplatin in Ferrets. Neuropharmacology. 1996; 35:1121–1129. [PubMed: 9121615]

7. Young JR, Eid R, Turner C, DeVita RJ, Kurtz MM, Tsao KLC, Chicchi GG, Wheeldon A, Carlson E, Mills SG. Pyrrolidine-Carboxamides and Oxadiazoles As Potent hNK$_1$ Antagonists. Bioorg Med Chem Lett. 2007; 17:5310–5315. [PubMed: 17723300]

8. Desai MC, Lefkowitz SL, Thadeio PF, Longo KP, Snider RM. Discovery of a Potent Substance P Antagonist: Recognition of the Key Molecular Determinant. J Med Chem. 1992; 35:4911–4913. [PubMed: 1282570]

9. Lewis RT, Macleod AM, Merchant KJ, Kelleher F, Sanderson I, Herbert RH, Cascieri MA, Sadowski S, Ball RG, Hoogsteen K. Tryptophan-Derived NK1 Antagonists: Conformationally Constrained Heterocyclic Bioisosteres of The Ester Linkage. J Med Chem. 1995; 38:923–933. [PubMed: 7699709]

10. Takeuchi Y, Berkley Shands EF, Beusen DD, Marshall GR. Derivation of a Three-Dimensional Pharmacophore Model of Substance P Antagonists Bound to the Neurokinin-1 Receptor. J Med Chem. 1998; 41:3609–3623. [PubMed: 9733486]

11. Yamamoto T, Nair P, Jacobsen NE, Kulkarni V, Davis P, Ma S, Navratilova E, Yamamura HI, Vanderah TW, Porreca F, Lai J, Hruby VJ. Biological and Conformational Evaluation of Bifunctional Compounds for Opioid Receptor Agonists and Neurokinin 1 Receptor Antagonists Possessing Two Penicillamines. J Med Chem. 2010; 53:5491–5501. [PubMed: 20617791]

12. Kalso E. Improving Opioid Effectiveness: From Ideas to Evidence. Eur J Pain. 2005; 9:131–135. [PubMed: 15737801]

13. King T, Gardell LR, Wang R, Vardanyen A, Ossipov MH, Malan TP Jr, Vanderah TW, Hunt SP, Hruby VJ, Lai J, Porreca F. Role of NK-1 Neurotransmission in Opioid-induced Hyperalgesia. Pain. 2005; 115:276–288. [PubMed: 15964684]

14. Armour DR, Aston NM, Morriss KML, Congreve MS, Hawcock AB, Marquess D, Mordaunt JE, Richards SA, Ward P. 1,4-Benzodiazepin-2-one Derived Neurokinin-1 Receptor Antagonists. Bioorg Med Chem Lett. 1997; 7:2037–2042.

15. Yamamoto T, Nair P, Vagner J, Largent-Milnes T, Davis P, Ma S, Navratilova E, Moye S, Tumati S, Lai J, Yamamura HI, Vanderah TW, Porreca F, Hruby VJ. A Structure-Activity Relationship Study and Combinatorial Synthetic Approach of C-terminal Modified Bifunctional Peptides That Are δ/μ Opioid Receptor Agonists and Neurokinin 1 Receptor Antagonists. J Med Chem. 2008; 51:1369–1376. [PubMed: 18266313]

16. Yamamoto T, Nair P, Ma SW, Davis P, Yamamura HI, Vanderah TW, Porreca F, Lai J, Hruby VJ. The Biological Activity and Metabolic Stability of Peptidic Bifunctional Compounds That Are Opioid Receptor Agonists And Neurokinin 1 Receptor Antagonists With a Cysteine Moiety. Bioorg Med Chem. 2009; 17:7337–7343. [PubMed: 19762245]

17. Ballet S, Pietsch M, Abell AD. Multiple Ligands in Opioid Research. Protein Pept Lett. 2008; 15:668–682. [PubMed: 18782061]

18. Lipkowski AW. Cooperative reinforcement of opioid pharmacophores. Polish J Pharmacol Pharm. 1987; 39:585–596.

19. Morphy R, Rancovic Z. Designed Multiple Ligands. An Emerging Drug Discovery Paradigm. J Med Chem. 2005; 48:6523–6543. [PubMed: 16220969]

20. Misterek K, Maszczynska I, Dorociak A, Gumulka SW, Carr DB, Szyfelbein SK, Lipkowski AW. Spinal co-administration of peptide substance P antagonist potentiates antinociceptive effect of opioid peptide. Life Sci. 1994; 54:939–944. [PubMed: 7511201]

21. Lipkowski, AW.; Carr, DB.; Misicka, A.; Misterek, K. Biological activities of a peptide containing both casomorphin-like and substance P antagonist structural characteristics. In: Brantl, V.; Teschemacher, H., editors. β-casomorphins and related peptides: Recent developments. VCH; Weinheim: 1994. p. 113-118.

22. Bonney IM, Foran SE, Marchand JE, Lipkowski AW, Carr DB. Spinal antinociceptive effects of AA501, a novel chimeric peptide with opioid receptor agonist and tachykinin receptor antagonist moieties. Eur J Pharmacol. 2004; 488:91–99. [PubMed: 15044040]

23. Ripley TL, Gadd CA, De Filipe C, Hunt SP, Stephens DN. Lack of Self- Administration and Behavioural Sensitization to Morphine, But Not Cocaine, in Mice Lacking NK1 Receptors. Neuropharmacology. 2002; 43:1258–1268. [PubMed: 12527475]

24. Morphy, R.; Rancovic, Z. Design of Multitarget Ligands. In: Rancovic, Z.; Morphy, R., editors. Lead Generation Approaches in Drug Discovery. John Wiley & Sons, Inc; Hoboken: 2010. p. 141-164.

25. Hruby VJ. Organic Chemistry and Biology: Chemical Biology Through the Eyes of Collaboration. J Org Chem. 2009; 74:9245–9264. [PubMed: 20000552]

26. Yamamoto T, Nair P, Vagner J, Davis P, Ma SW, Navratilova E, Moye S, Tumati S, Lai J, Yamamura HI, Vanderah TW, Porreca F, Hruby VJ. Design, Synthesis, And Biological Evaluation
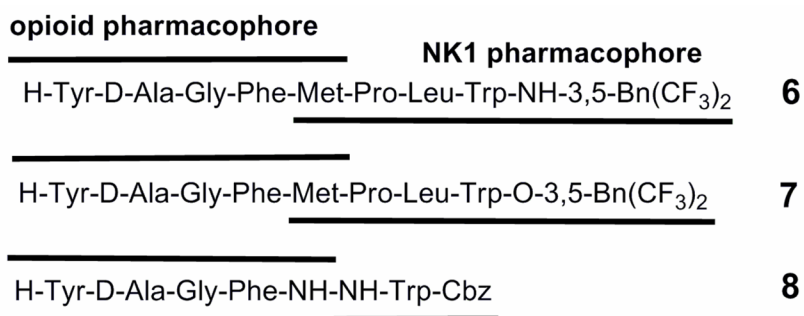
of Novel Bifunctional C-terminal-Modified Peptides for δ/μ Opioid Receptor Agonists and Neurokinin-1 Receptor Antagonists. J Med Chem. 2007; 50:2779–2786. [PubMed: 17516639]

27. Yamamoto T, Nair P, Jacobsen NE, Davis P, Ma SW, Navratilova E, Moye S, Lai J, Yamamura HI, Vanderah TW, Porreca F, Hruby VJ. The Importance of Micelle-Bound States for the Bioactivities of Bifunctional Peptide Derivatives for δ/μ Opioid Receptor Agonists and Neurokinin 1 Receptor Antagonists. J Med Chem. 2008; 51:6334–6347. [PubMed: 18821747]

28. Largent-Milnes TM, Yamamoto T, Nair P, Moulton JW, Hruby VJ, Lai J, Porreca F, Vanderah TW. Spinal or Systemic TY005, A Peptide Opioid Agonist/Neurokinin 1 Receptor Antagonist, Attenuates Pain With Reduced Tolerance. Br J Pharmacol. 2010; 161:986–1001. [PubMed: 20977451]

29. Van den Eynde I, Laus G, Schiller PW, Kosson P, Chung NN, Lipkowski AW, Tourwé D. A New Structural Motif for Mu Opioid Antagonists. J Med Chem. 2005; 48:3644–3648. [PubMed: 15887972]

30. Ballet S, Feytens D, De Wachter R, De Vlaeminck M, Marczak ED, Salvadori S, de Graaf C, Rognan D, Negri L, Lattanzi R, Lazarus LH, Tourwé D, Balboni G. Conformationally Constrained Opioid Ligands: The Dmt-Aba and Dmt-Aia versus Dmt-Tic Scaffold. Bioorg Med Chem Lett. 2009; 19:433–437. [PubMed: 19062273]

31. Ballet S, De Wachter R, Van Rompaey K, Tomboly Cs, Feytens D, Toth G, Quartara L, Cucchi P, Meini S, Tourwé D. Bradykinin Analogues Containing The 4- Amino-2-Benzazepin-3-one Scaffold at the C-Terminus. J Pept Sci. 2007; 13:164–170. [PubMed: 17266049]

32. Feytens D, Cescato R, Reubi JC, Tourwé D. New sst(4/5)-selective Somatostatin Peptidomimetics Based on a Constrained Tryptophan Scaffold. J Med Chem. 2007; 50:3397–3401. [PubMed: 17559206]

33. Feytens D, De Vlaeminck M, Cescato R, Tourwé D, Reubi JC. Highly Potent 4-Amino-Indolo[2,3-c]Azepin-3-One-Containing Somatostatin Mimetics With a Range of sst Receptor Selectivities. J Med Chem. 2009; 52:95–104. [PubMed: 19067538]

34. Schiller PW, Nguyen TMD, Berezowska I, Dupuis S, Weltrowska G, Chung NN, Lemieux C. Synthesis and In Vitro Opioid Activity Profiles of DALDA Analogues. Eur J Med Chem. 2000; 35:895–901. [PubMed: 11121615]

35. Ballet S, Urbanczyk-Lipkowska Z, Tourwé D. Synthesis of Substituted 4-Amino-2-Benzazepin-3-Ones Via N-Acyliminium Ion Cyclizations. Synlett. 2005:2791–2795.

36. Mondini, S.; Dall Avo, M.; Guerrato, A. Process for the Preparation of 3,5- Bistrifluoromethyl-N-Methylbenzylamine. WO2007107818(A2). 2008.

37. Tourwé D, Verschueren K, Frycia A, Davis P, Porreca F, Hruby VJ, Toth G, Jaspers H, Verheyden P, Van Binst G. Conformational Restriction of Tyr and Phe Side Chains in Opioid Peptides: Information About Preferred and Bioactive Side-Chain Topology. Biopolymers. 1996; 38:1–12. [PubMed: 8679939]

38. Iterbeke K, Laus G, Verheyden P, Tourwé D. Lett Pept Sci. 1998; 5:121.Millet R, Goossens JF, Bertrand-Caumont K, Chavatte P, Houssin R, Hénichart JP. Lett Pept Sci. 1999; 6:221.

39. Cascieri MA, Macleod AM, Underwood D, Shiao LL, Ber E, Sadowski S, Yu H, Merchant KJ, Swain CJ, Strader CD, Fong TM. Characterization of the Interaction of N-Acyl-L-Tryptophan Benzyl Ester Neurokinin Antagonists With the Human Neurokinin-1 Receptor. J Biol Chem. 1994; 269:6587–6591. [PubMed: 7509807]

40. Janecka A, Poels J, Fichna J, Studzian K, Vanden Broeck J. Comparison of Antagonist Activity of Spantide Family at Human Neurokinin Receptors Measured by Aequorin Luminescence-Based Functional Calcium Assay. Regul Pept. 2005; 131:23– 28. [PubMed: 15990182]

41. Schild HO. pA$_2$, A New Scale For The Measurement of Drug Antagonism. Br J Pharmacol. 1947; 2:189–206.

42. Arunlakshana O, Schild HO. Some Quantitative Uses of Drug Antagonists. Br J Pharmacol Chemother. 1959; 14:45–58.

43. Ballet S, Frycia A, Piron J, Chung NN, Schiller PW, Kosson P, Lipkowski AW, Tourwé D. Synthesis and Biological Evaluation of Constrained Analogues of the Opioid Peptide H-Tyr-D-Ala-Phe-Gly-NH$_2$ Using the 4-Amino-2-Benzazepin-3-One Scaffold. J Pept Res. 2005; 66:222–230. [PubMed: 16218989]

44. Ballet S, Misicka A, Kosson P, Lemieux C, Chung NN, Schiller PW, Lipkowski AW, Tourwé D. Blood-Brian Barrier Penetration By Two Dermorphin Tetrapeptide Analogues: Role of Lipophilicity vs. Structural Flexibility. J Med Chem. 2008; 51:2571–2574. [PubMed: 18370374]

45. Ballet S, Marczak ED, Feytens D, Salvadori S, Sasaki Y, Abell AD, Lazarus LH, Balboni G, Tourwé D. Novel Multiple Opioid Ligands Based on 4-Aminobenzazepinone (Aba), Azepinoindole (Aia) and Tetrahydroisoquinoline (Tic) Scaffolds. Bioorg Med Chem Lett. 2010; 20:1610–1613. [PubMed: 20137938]

46. Tourwé D, Verschueren K, Van Binst G, Davis P, Porreca F, Hruby VJ. Dermorphin Sequence With High Delta Affinity By Fixing the Phe Side-chain to Trans at Alfa-1. Bioorg Med Chem Lett. 1992; 2:1305–1308.

47. Schiller PW. Bi- or Multifunctional Opioid Peptide Drugs. Life Sci. 2010; 86:598–603. [PubMed: 19285088]

48. Zhao K, Luo G, Zhao GM, Schiller PW, Szeto HH. Transcellular Transport of a Highly Polar 3+ Net Charge Opioid Tetrapeptide. J Pharmacol Exp Ther. 2003; 304:425–432. [PubMed: 12490619]

49. Cheng YC, Prusoff WH. Relationship Between the Inhibition Constant (Ki) and the Concentration of Inhibitor Which Causes 50 per cent (I_{50}) of an Enzymatic Reaction. Biochem Pharmacol. 1973; 22:3099–3108. [PubMed: 4202581] 46 Paton WDM. The Action of Morphine and Related Substances on Contraction and on Acetylcholine Output of Coaxially Stimulated Guinea-pig ileum. Br J Pharmacol Chemother. 1957; 12:119–127. [PubMed: 13413163]

50. Henderson G, Hughes J, Kosterlitz HW. A New Example of a Morphine-Sensitive Neuro-Effector Junction: Adrenergic Transmission in the Mouse Vas Deferens. Br J Pharmacol. 1972; 46:764–766. [PubMed: 4655272]

51. Schiller PW, Lipton A, Horrobin DF, Bodansky M. Unsulfated C-Terminal 7- Peptide of Cholecystokinin: A New Ligand of the Opiate Receptor. Biochem Biophys Res Commun. 1978; 85:1332–1338. [PubMed: 217386]

52. DiMaio J, Nguyen TMD, Lemieux C, Schiller PW. Synthesis and Pharmacological Characterization in Vitro of Cyclic Enkephalin Analogues: Effect of the Conformational Constraints on Opioid Receptor Selectivity. J Med Chem. 1982; 25:1432–1438. [PubMed: 6296388]

53. Waterfield AA, Leslie FM, Lord JAH, Ling N, Kosterlitz HW. Opioid Activities of Frangments of β-Endorphin and Its Leucine[5]-Analogue. Comparison of the Binding Properties of Methionine- and Leucine-Enkephalin. Eur J Pharmacol. 1979; 58:11–18. [PubMed: 499333]

54. Mohamadi F, Richards NGJ, Guida WC, Liskamp R, Lipton M, Caufield C, Chang G, Hendrickson T, Still WC. Macromodel - An Integrated Software System for Modeling Organic and Bioorganic Molecules Using Molecular Mechanics. J Comp Chem. 1990; 11:440–467.

55. Allinger NL, Yuh YH, Lii JH. Molecular Mechanics - The MM3 Force-field for Hydrocarbons 1. J Am Chem Soc. 1989; 111:8551–8566.

56. Still WC, Tempczyk A, Hawley RC, Hendrickson T. Semianalytical Treatment of Solvation for Molecular Mechanics and Dynamics. J Am Chem Soc. 1990; 112:6127–6129.

57. Kolossvary I, Guida WC. Low mode search. An efficient, automated computational method for conformational analysis: Application to Cyclic and Acyclic Alkanes and Cyclic Peptides. J Am Chem Soc. 1996; 118:5011–5019.
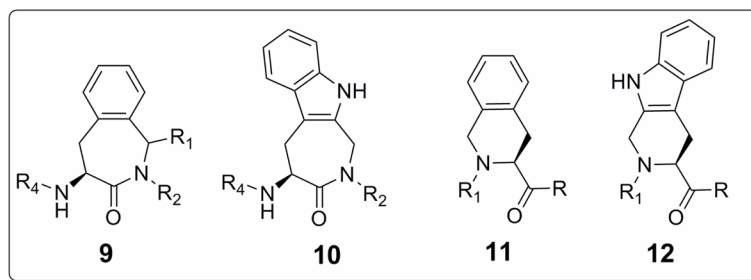
Figure 1.
Structures of reported peptidomimetic NK1R antagonists

opioid pharmacophore

NK1 pharmacophore

H-Tyr-D-Ala-Gly-Phe-Met-Pro-Leu-Trp-NH-3,5-Bn(CF$_3$)$_2$ **6**

H-Tyr-D-Ala-Gly-Phe-Met-Pro-Leu-Trp-O-3,5-Bn(CF$_3$)$_2$ **7**

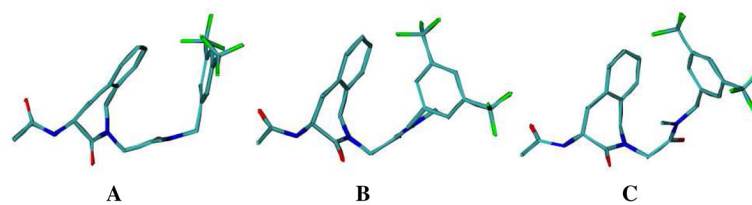H-Tyr-D-Ala-Gly-Phe-NH-NH-Trp-Cbz   **8**

Figure 2.
Examples of reported bifunctional opioid-NK1 ligands **6**, **7** and **8**.

Figure 3.
General structures of the 4-amino-1,2,4,5-tetrahydro-2-benzazepin-3-one **9** (Aba), amino indoloazepinone **10** (Aia), tetrahydroisoquinoline **11** (Tic) and tetrahydro-β-carboline **12** (Tcc) scaffolds.

Figure 4.
The three lowest energy conformations of compound **20** showing a stacked orientation of the aromatics (A), a T-perpendicular orientation (B, 3.94 kJ/mol above A) and a L-perpendicular orientation
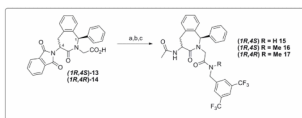
Scheme 1.
Synthesis of 1-phenyl Aba analogues **15** to **17**.
Reaction conditions: a) 1.1 eq. 3′,5′-bistrifluoromethyl benzylamine or *N*-methyl-3′,5′-bistrifluoromethyl benzylamine, 1.1 eq. TBTU, 3 eq. TEA, CH_2Cl_2, r.t. 2h; b) 2 eq. $NH_2NH_2.H_2O$, EtOH, reflux, 1.5h; c) 5 eq. Ac_2O, TEA, EtOH, r.t., 3h.
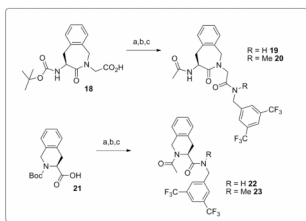
Scheme 2.
Synthesis of Aba and Tic analogues 19, 20, 22 and 23.
Reaction conditions: a) 1.1 eq. 3′,5′-bistrifluoromethyl benzylamine or *N*-methyl-3′,5′-bistrifluoromethyl benzylamine, 1.1 eq. TBTU, 3 eq. TEA, CH$_2$Cl$_2$, r.t. 2h; b) TFA/CH$_2$Cl$_2$/anisole 49:49:2, r.t. 3h; c) 5 eq. Ac$_2$O, TEA, EtOH, r.t., 3h.
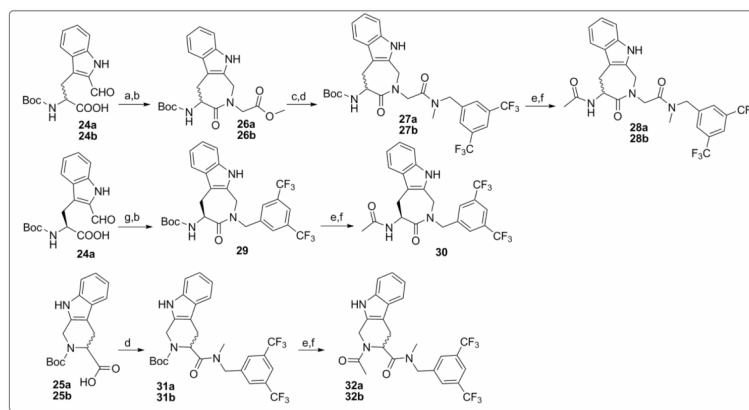
Scheme 3.
Synthesis of Aia and Tcc analogues **28a/b**, **30** and **32a/b**.

Reaction conditions: a) 1.05 eq. H-GlyOMe.HCl, 20 wt% MgSO$_4$, 2.5 eq. NaBH$_3$CN, CH$_2$Cl$_2$, pH 6, r.t., 4h; b) 1.5 eq. EDC.HCl, 2.5 eq. pyridine, acetonitrile:water 1:1, r.t., 2 days; c) 4 eq. 1M aq. LiOH, MeOH, r.t., 1.5h; d) 1.1 eq. *N*-methyl-3′,5′-bistrifluoromethyl benzylamine, 1.1 eq. TBTU, 3 eq. NEt$_3$, r.t., 2h; e) 5% H$_2$O in TFA:acetonitrile 4:1, r.t., 1h; f) acetonitrile:H$_2$O 1:1, NEt$_3$, pH 6, 5 eq. Ac$_2$O, r.t., 2h; g) 1.05 eq. 3′,5′-bistrifluoromethyl benzylamine, 20 wt% MgSO$_4$, 2.5 eq. NaBH$_3$CN, CH$_2$Cl$_2$, pH 6, r.t., 4h.
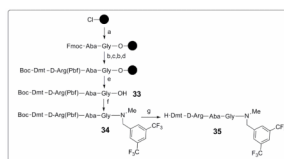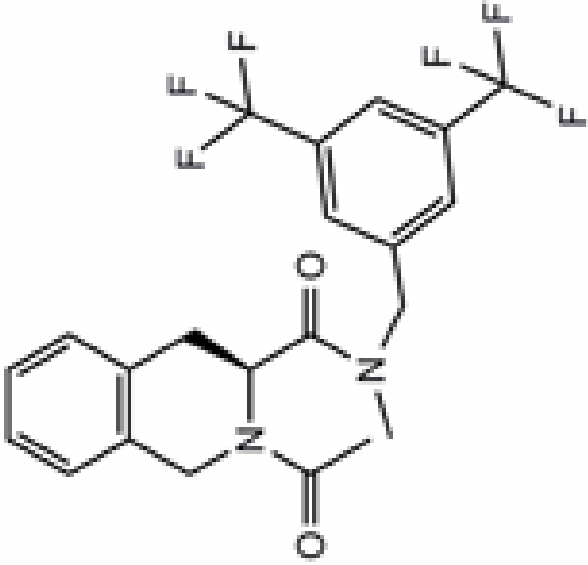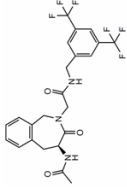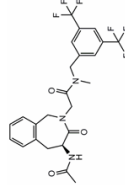
Scheme 4.
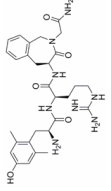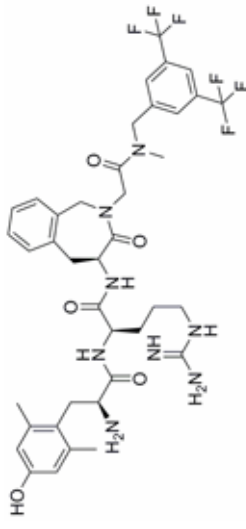Synthesis of bifunctional chimera **35**.
Reaction conditions: a) Fmoc-Aba-Gly-OH, diisopropylethylamine, CH$_2$Cl$_2$, r.t., overnight; b) 20% piperidine/DMF (5min+15min); c) Coupling of Fmoc-D-Arg(Pbf)-OH and DIC/HOBt in DMF r.t., 2h; d) Coupling of Boc-Dmt-OH and DIC/HOBt in DMF r.t., 2h; e) 1% TFA in CH$_2$Cl$_2$ for 30 min; f) Coupling of *N*-methyl-3′,5′-bistrifluoromethyl benzylamine with BOP/DIPEA in DMF, r.t., 3h; g) TFA/CH$_2$Cl$_2$/anisole 49:49:2, r.t., 2h.

Table 1

Structures, functional activities and affinities of NK1-, opioid- and opioid-NK1 ligands

Structure	Comp.	NK1R pA₂[a]	hNK1R Kᵢ (nM)[b]	GPI(μ) IC₅₀ (nM) [c]	MVD(δ) IC₅₀ (nM) [c]	MOR Kᵢ (nM) [c]	DOR Kᵢ (nM)[c]	KOR Kᵢ (nM) [c]
	23	7.5	32±4	/	/	/	/	/
	19	6.2	387±66	/	/	/	/	/
	20	8.4	27±4	/	/	/	/	/

Comp.	Structure	NK1R pA$_2$[a]	hNK1R K$_i$ (nM)[b]	GPI(μ) IC$_{50}$ (nM) [c]	MVD(δ) IC$_{50}$ (nM) [c]	MOR K$_i$ (nM) [c]	DOR K$_i$ (nM)[c]	KOR K$_i$ (nM) [c]
36		/	/	0.32 ± 0.04	0.42 ± 0.02	0.15 ± 0.02	0.60 ± 0.07	118 ± 12
35		7.8	0.5±0.1	8.51 ± 0.62	43.3 ± 6.3	0.416 ± 0.012	10.4± 0.6	445 ± 81

[a] The pA2 values were calculated using the Schild's equation.[41]

[b] Inhibitory constants (K$_i$) of NK1 receptor ligands, measured for the receptor prototype [^{3}H]-SP in the presence of hNK1-CHO membranes. Results are means ± SEM of three independent experiments. Binding data were calculated using the nonlinear regression/one site competition fitting options of the GraphPad Prism Software.

[c] Values represent means of 3–6 experiments ± SEM. The GPI functional assay is representative of MOR activation, whereas the MVD is a δ receptor-representative assay. Binding affinities of compounds for μ and δ opioid receptors were determined by displacing [^{3}H]DAMGO and [^{3}H]DSLET, respectively, from rat brain membrane binding sites and binding affinities for κ opioid receptors were measured by displacement of [^{3}H]U69,593 from guinea pig brain membrane binding sites.